The Mössbauer Effect

Sahar Khashayar[1, *] and Em Mcglone[1, †]

[1] *Department of Physics, Harvard University, Cambridge, Massachusetts 02138, USA*

(Dated: December 10, 2021)

The Mössbauer effect refers to the recoil-free emission and absorption of gamma rays in a solid. It is used to probe properties of the lattice surrounding the absorbing or emitting nucleus. In this experiment, we used a ^{57}Co radioactive source to measure the Mössbauer effect in stainless steel, yttrium iron garnet, and FeF_2 to observe the isomer/chemical shift, temperature shift, and the transition to antiferromagnetism.

I. INTRODUCTION

The nuclei of atoms have quantized energy levels, and can absorb or emit photons as they transition between energy levels. These transitions usually occur via a process known as recoil emission: in recoil emission, the nucleus must carry momentum equal and opposite to the momentum of the emitted gamma ray. The nucleus's kinetic energy takes up some of the energy from the transition, thus leaving less energy for the emitted gamma ray. The gamma ray therefore has a lower energy than the energy released by the transition.

Similarly, absorption with nuclear recoil absorbs a gamma ray of greater energy than the transition energy, since the kinetic energy of the nucleus will also take up some of the energy in the interaction.

The Mössbauer effect, as discovered by Rudolph Mössbauer in 1958, refers to the recoil-free emission and absorption of gamma rays by nuclei in a solid. The recoil momentum is absorbed by the entire lattice of the solid surrounding the nucleus, thus making the kinetic energy of the individual nucleus effectively zero [1] [2].

These gamma rays carry a very narrow, well-defined energy, and the emission and absorption lines overlap. This means they are very sensitive to small changes in the energies of nuclear transitions. Because of this, gamma rays can be used as a probe to observe interactions between a nucleus and its electrons and those of its neighbors [3]. This is the basis for Mössbauer spectroscopy, which combines the Mössbauer effect with the Doppler effect to monitor such interactions.

The velocity of the emitter will affect the energy shift in the gamma ray due to the Doppler effect. Observing this shift at different velocities/energies can provide information on the environment surrounding the nucleus. In our experiment, we observed the isomer shift, second order Doppler shift as a result of temperature shift, as well as the antiferromagnetic transition at cold temperatures.

* skhashayar@college.harvard.edu

† mdmcglone@college.harvard.edu

A. Isomer (Chemical) Shift

The isomeric shift as seen in Mössbauer spectroscopy refers to the frequency shift of the gamma ray spectral lines that occurs when compares two different nuclear isomeric states in two different environments. It is caused by the combined effect of the recoil-free Mössbauer transition between the two nuclear isomeric states and the transition between two atomic states in those two environments.

The electrons surrounding the nucleus have a probability of being found within the nuclear volume. The overlap between the electrons and the nucleus produces a change in energy due to Coulomb interaction, and this in turn changes the total energy of the system. The overlap between different energy states of the nuclei will be different depending on the radii of the nuclei in that, and so the isomer shift will also be measurably different [4]. Thus, Mössbauer spectra are never exactly centered about zero energy shift, or zero velocity, but are always shifted slightly.

In this experiment, we observed the shift between our ^{57}Fe source and ^{57}Fe in various absorbers: iron, stainless steel, yttrium iron garnet ($Y_3Fe_5O_{12}$), cyanide ($Na_4[Fe(CN)_6]\cdot 10H_2O$), and FeF_2.

B. Temperature Shift

The thermal vibrations of nuclei can shift the frequency of their recoil free radiation by means of the relativistic Doppler effect [5]. If the nucleus is moving with a velocity v, an observer in the lab frame perceives a nuclear-frame clock to run slow according to the following equation:

$$\sqrt{1-\left(\frac{v}{c}\right)^2} \tag{1}$$

Since $\langle v\rangle^2$ increases with temperature, the Mössbauer shifts get lower with a decrease in temperature. [6].

We cool the FeF_2 with liquid nitrogen in order to measure these shifts.

C. Antiferromagnetism

The iron atom undergoes a transition to ferromagnetic or antiferromagnetic order at much lower temperatures [7], close to 70K. Antiferromagnetism refers to a material in which the magnetic moments or spins of neighboring particles in a lattice align in a pattern of pointing in opposite directions. Thus, the nuclear spin of the iron atoms will interact with the magnetization of the surrounding lattice. These interactions split the ground and excited states, and we can observe the splitting of these energy levels to determine the magnetization of the surrounding lattice. In either case, the net magnetization is zero; however, in an antiferromagnetic material, the field on the hyperfine level is nonzero.

By pumping on the liquid nitrogen, we can cool the target down to 60K, and in the intervening temperatures see the transition to antiferromagnetism.

II. SETUP/APPARATUS

The Apparatus includes the following:

- ^{57}Co source (in palladium matrix) mounted on velocity driver (loudspeaker)
- velocity transducer (Sanborn LVsyn 6LV2)
- driver control unit
- proportional counter (Reuter-Stokes RSG-61) with H.V. power supply (Ortec 478)
- proportional counter preamp (Canberra 806)
- spectroscopy amplifier (Ortec 570)
- single channel analyzer (Ortec 551)
- linear gate and pulse stretcher (Ortec 542)
- multichannel analyzer (computer-based)
- National Instruments PCI-6070E interface card
- oscilloscope (Tektronix 2225)
- universal counter (Hewlett Packard 5315A)
- liquid nitrogen cryostat (Precision Cryogenic Systems PCS 4-06-102) with cold finger
- mechanical vacuum pump
- temperature controller (Lake Shore 330)
- Michelson interferometer for velocity calibration (5 mW HeNe laser, beam splitter, mirrors and photodetector)
- various absorbers, including Fe enriched in ^{5}7Fe, Fe_2O_3 (ferric oxide), $Na_4Fe(CN)_6{\cdot}10H_2O$ (sodium ferrocyanide), FeF_2 (ferrous fluoride), stainless steel (thicknesses from 0.2 to 3 mils), garnet, and others

A. Radioactive Source

The radioactive source is ^{57}Co in a Pd matrix with a diameter of 6 mm. It has a half life of 270 days, and decays by K-electron capture to ^{57}Fe. It is contained in a lead shield. The source strength was 4.5 mCi as of December 2019.

B. Velocity Driver/Transducer and Driver Control unit

The velocity driver is a loudspeaker which is driven harmonically by a sinusoidal voltage supplied by a driver control unit. The connecting rod between the ^{57}Co source and the loudspeaker is a LVsyn velocity transducer. It consists of a shielded cylindrical coil assembly and a permanent magnet. The relative motion of the magnet and the coil generates a voltage whose magnitude is proportional to the velocity. The driver control unit is a precision oscillator and amplifier. It provides the 10-100 Hz sinusoidal driving voltage for the loudspeaker. The trigger signal is used to start the sweep of the multichannel scaler. The phase of the trigger out can be set to 0° or 90° with respect to the amp out, or any value in between with the delay adjust. This makes it is possible to select at which point one wants the MCS sweep to begin with respect to the motion of the source. Simultaneous display of the LVsyn and trigger signals on the scope facilitates this adjustment.

C. Detector

The detector is a proportional counter with a 1-inch diameter, 0.010-inch thick (46 mg/cm2), beryllium side window. The counter is filled with a mixture of Xe-CO^2 gas at one atmosphere pressure. The bias voltage (+1850 V) is supplied by a High Voltage power supply. It is fed through the preamplifier to the counter.

D. Preamp, Amplifier and Single Channel Analyzer

The proportional counter signal is first amplified and buffered by the preamplifier before it goes to the amplifier. The spectroscopy amplifier further amplifies and shapes the signal. Then, the signal is routed to the multichannel analyzer (MCA) and the single channel analyzer (SCA). The SCA is used to sort out those pulses corresponding to the 14 keV gamma rays.

E. LabVIEW Multichannel Analyzer

The MCA has two modes of operation: pulse height analysis (PHA) or multichannel scaling (MCS). In the PHA mode it stores a histogram of pulses its input sees versus the voltage of those pulses, which is proportional to the energy of the gamma ray. The PHA will be used to view the energy spectrum of the source and to select the 14 keV line. MCS mode stores a histogram of pulses its input sees versus time. The MCS advances repeatedly through a set time period split up into many time bins and stores the number of counts received during each

time bin in that particular bin. By harmonically moving the ^{57}Co source and monitoring the counts from the proportional counter, the MCS provides a histogram of counts versus velocity of the ^{57}Co source.

F. Liquid Nitrogen Cryostat

The two-liter liquid nitrogen cryostat contains an iron flouride sample on a temperature-controlled copper rod. The iron fluoride is in powder form, and is mixed with silicone grease. The sample is located between two beryllium windows to thermal insulate the sample without significantly attenuating the gamma rays from the source. A vacuum manifold is attached to the cryostat jacket and liquid nitrogen container. Liquid nitrogen can cool the sample to its boiling point at 77.3k, and pumping the container can reduce the temperature to 60k. The vacuum jacket is maintained below 30 mTorr to thermally insulate the liquid nitrogen container. A copper cold finger is mounted in the bottom of the liquid container. It is connected to the sample through a calibrated copper wire, which sets the time constant for cooling at about 25 minutes. A platinum resistance thermometer measures the temperature near the sample. The Lake Shore 330 temperature controller supplies current to a heater, which is a 25 Ω resistor, in order to have the sample reach a set temperature.

G. Michelson Interferometer

The velocity of the driver and source has to be calibrated in order to calculate the Doppler shift of the gamma rays. The Michelson interferometer is used to measure the displacement in units of the wavelength of light, and thus accurately determine the velocity of the source. This interferometer has two arms – one ending with a fixed mirror and another ending with a moving mirror, which is next to the source. The two beams combine at a photodetector, producing interference fringes. The reflected and the incedent beams are split at a 50/50 beamsplitter cube. The source of coherent light is a 632.8 nm wavelength HeNe laser. We do a rough alignment using the laser beams, aligning the source holder with the interferometer.

H. Entire Setup

Overall, the Mössbauer apparatus operates as such: the velocity driver (loudspeaker) oscillates the radioactive source in proportion to the input voltage. The ^{57}Co source emits gamma rays with a range of small Doppler shifts related to the motion induced by the velocity driver. These gamma rays are either absorbed by or pass through the chosen absorber material depending on the absorber's resonant energies. The proportional counter counts the gamma rays that pass through the absorber. This data is processed through the preamplifier, amplifier, and SCA and exported to the computer where it may be viewed in either the PHA or MCS. The liquid nitrogen cryostat may also be used to control the temperature of an FeF_2 absorber. Figure 1 contains a schematic of the entire setup.

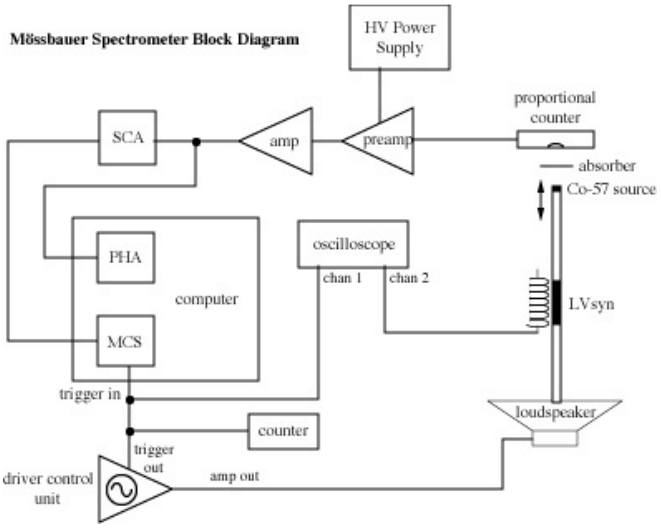

FIG. 1: A block diagram of all the parts of the Mössbauer spectroscopy setup.

III. EXPERIMENT

We first used the Michelson Interferometer to calibrate the velocity of the driver and ^{57}Co source in order to calculate the Doppler Shift of the source's gamma rays. We read the interferometer's output on an oscilliscope. The oscilliscope also displayed the input voltage for the velocity driver. At max input voltage, the velocity driver reaches its max speed. So, we counted a number of fringes of the waveform of the HeNe laser around the max voltage, and the time elapsed in these fringes, and used the following equation to calculate the max velocity of the velocity driver:

$$V_{\max} = \frac{(\text{number of fringes}) * \lambda_{\text{HeNe}}}{2 * t_{\text{elapsed}}} \tag{2}$$

This process was repeated for ten max input voltages so that we could calculate the velocity of the driver at any viable input voltage. The results are shown in Figure 2. The voltage input remained at 200 mV for the remainder of the experiment. The max velocity at this voltage was 17.4 mm/s, and the period of the oscillation was 20.875.

We then viewed in the PHA the emission spectrum of the ^{57}Co radioactive source. The ^{57}Co source in a Pd matrix emits a 6 keV line from an Fe x-ray, the 14.41 keV gamma line of interest, a 22 keV Pd x-ray, an 89

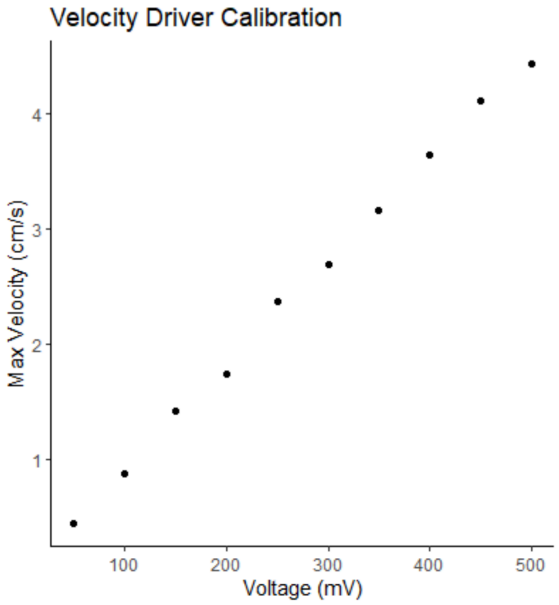

FIG. 2: The relation between input voltage and max velocity driver velocity as obtained through interferometry and Equation 2. The equation of the line is Max Velocity = $9.03{*}10^{-3}{*}$Voltage

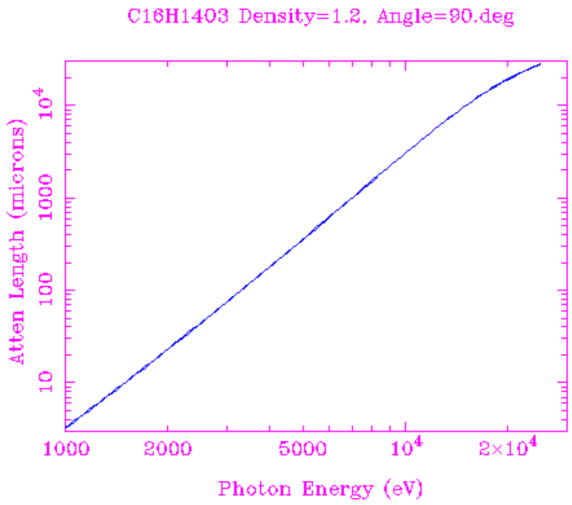

FIG. 3: X-ray attenuation length through polycarbonate at different energies as obtained from [**?**]

keV Pb x-ray, and 122 keV and 136 keV gamma lines from ^{57}Co. With no scattering target, the PHA displayed three evenly spaced emission lines. Since the amplifier cuts out higher energy events, it was likely that these lines were the 6 and 22 keV x-rays and the 14.41 keV gamma ray. The ratios between these lines supported this hypothesis, but to confirm it, we tested what kind of emission each line was using their attenuation lengths. First, we used the Atomic and Nuclear Data Tables from [8] to calculate the expected x-ray attenuation lengths in polycarbonate. According to Figure 3, as obtained from [8], the 6 keV x-ray should be able to travel through 0.04 cm of polycarbonate, and the 22 keV should be able to travel through 2 cm of polycarbonate. The 14.41 keV gamma ray should not be attenuated by polycarbonate. Then, we placed a 0.16 cm thick polycarbonate target between the ^{57}Co source and the detector. With this setup, the lowest energy line disappeared, providing evidence that this line is the 6 keV x-ray. Stacking five targets provided a 0.8 cm polycarbonate target. With this setup, the lowest energy line remained absent, and the highest energy line was reduced significantly, showing that the highest line is likely the 22 keV x-ray. The middle emission line was never attenuated, showing that it is in fact the 14.41 keV gamma ray line of interest. The SCA window was then adjusted accordingly to only record pulses corresponding to the 14.41 keV gamma ray line.

The MCS recorded the 14.41 keV gamma rays from the source in periods of 20 ms split up into 1000 time bins. This period is slightly less than the 20.875 ms period of the oscillation of the velocity driver so that the MCS does not skip any part of the oscillation. The period recorded in the MCS can be converted into the velocity in mm/s of the loudspeaker using the following equation:

$$V = -17.4 * cos((t + 0.0781)\frac{2\pi}{20.875}) \qquad (3)$$

Where t is the time bin recorded by the MCS, 17.4 is the max velocity in mm/s of the velocity driver, 20.875 is the period of the velocity driver's oscillation, and 0.0781 ms is time difference between the first minimum of the velocity driver's oscillation and the first trigger pulse of the MCS. The negative sign and cosine function are selected to match the oscillation of the input voltage, which starts near a minimum and increases initially.

A. Isomer (Chemical) Shift

By placing each absorber between the source and proportional counter, we looked at the Mössbauer spectra for the following absorber materials: stainless steel, yttrium iron garnet, FeF_2. All were measured at room temperature. The data resolution for stainless steel is worse than for the other materials because it was not tested as long; the stainless steel was tested for two hours, whereas the yttrium iron garnet was tested for 3.5 days, and the FeF_2 for 2.5 days. The Mössbauer spectra of the absorbers at the first velocity zero are shown in Figure 4. An image of the Mössbauer spectra refactored to display gamma ray counts received in relation to velocity is shown in Figure 5. Images of the whole Mössbauer spectra and the Mössbauer spectra at the second zero of the source's velocity for each absorber is included in the Appendix in Figures 8 and 9.

The dips in each of the spectra indicate where there are fewer counts of gamma rays in the proportional counter.

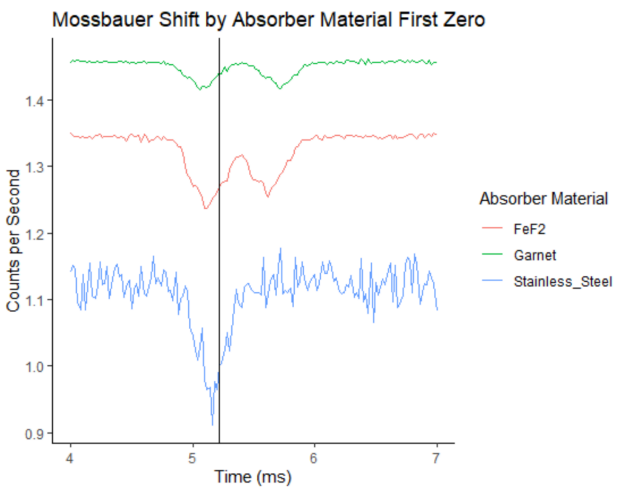

FIG. 4: Mössbauer spectra of different absorber materials. The black line is at time = 5.22 ms, the first zero of velocity of the loudspeaker based on the period of 20.875 ms. Dips represent Doppler shifts at which the gamma rays had energies resonant with the material. Multipliers applied to order material lines: Garnet/1.5, FeF_2*1, Stainless Steel*1.05

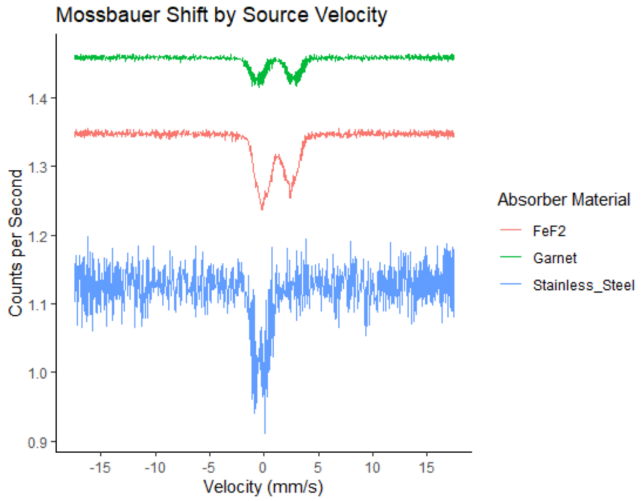

FIG. 5: Mössbauer spectra of different absorber materials in relation to source velocity. Dips represent Doppler shifts at which the gamma rays had energies resonant with the material. Multipliers applied to order material lines: Garnet/1.5, FeF_2*1, Stainless Steel*1.05

This occurs at the Doppler shifts where more of the gamma rays are being absorbed by the material. These resonant energy absorption peaks occur not quite at the zeros of velocity, but at a slight shift depending on material (as shown in this section) and temperature (as discussed next). The time bins of the spectral dips were found using findpeaks() in R. The time was then converted to a source velocity using Equation 3. Using the following equation, the source velocities at which the gamma rays were resonant with the material were converted to an energy shift.

$$\Delta E = \frac{V}{c} E \tag{4}$$

Where ΔE is the energy shift, V is the velocity of the source, c is the speed of light, and E is the initial emitted energy (14.41 keV). The energy shift added with the initial energy of 14.41 keV defines the resonant absorbtion energy. The materials displayed different resonant absorbtion energies, as listed in Table I.

B. Temperature Shift

Using the FeF_2 absorber and the liquid nitrogen cryostat, we cooled the absorber down to several different temperatures: room temperature (300K), 190K, 85K, 78K, 70K and 65K. We can observe the shift in the peaks through all of these different temperatures. The Mössbauer spectra at the first zero of the source's velocity of all the tested temperatures are shown in Figure 6. The Mössbauer spectra refactored to display gamma ray counts received in relation to velocity is shown in Figure 7. The whole Mössbauer spectra and the Mössbauer spectra at the second zero of the source's velocity of all the tested temperatures are shown in the Appendix in Figures 10 and 11.

The same process using Equation 4 was used as in the Isomer Shift section to calculate the resonant energy shifts at each temperature. The energy shifts of the temperatures above the Néel transition are listed in Table II.

C. Antiferromagnetism

In addition, when the temperatures drop below the Néel transition at around 78K, the FeF_2 absorber becomes antiferromagnet. This causes the total magnetization of the material to become zero, but on a smaller scale and at a local level around individual nuclei, we can see the effects of the neighboring nuclei's magnetic fields. This is visible in Figure 7, the image of the whole Mössbauer spectra of the FeF_2 at different temperatures.

IV. CONCLUSIONS

A. Isomer Shift

We indeed observed a different energy shift in the Mössbauer spectrum for each of the different materials, as illustrated in Figure 8 and Table I.

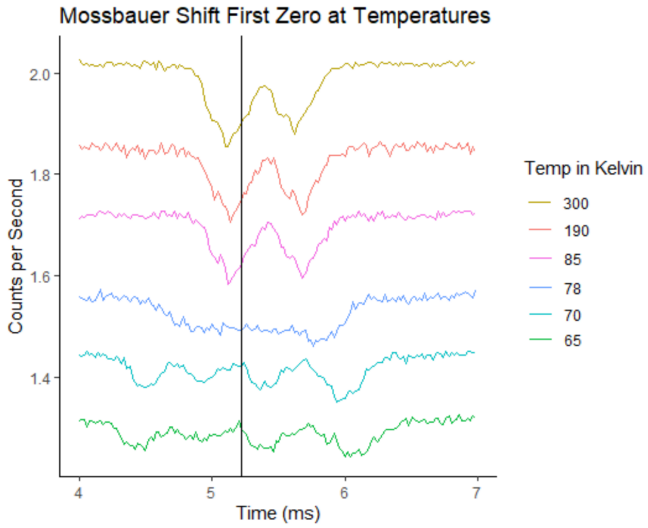

FIG. 6: Mössbauer spectra of FeF_2 absorber at different temperatures. The black line is at time = 5.22 ms, the first zero of velocity of the loudspeaker based on the period of 20.875 ms. Dips represent Doppler shifts at which the gamma rays had energies resonant with the material. Multipliers applied to order temperature lines: 300k*1.5, 190k*1.32, 85k*1.2, 78k*1.1, 70k/1.1, 65k/1.1.

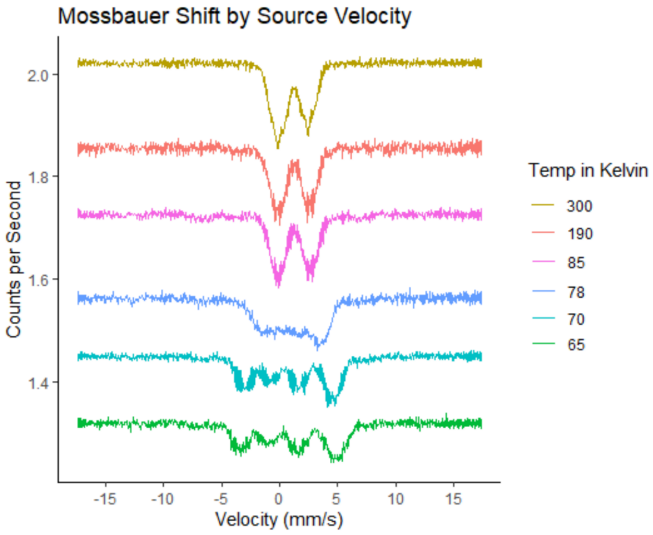

FIG. 7: Mössbauer spectra of FeF_2 absorber at different temperatures in relation to source velocity. Dips represent Doppler shifts at which the gamma rays had energies resonant with the material. The two dips split into four as the absorber goes below the Néel transition at 78k. Multipliers applied to order temperature lines: 300k*1.5, 190k*1.32, 85k*1.2, 78k*1.1, 70k/1.1, 65k/1.1.

B. Temperature Shift

The shifts of the middle two peaks remain largely unchanged at different temperatures, as shown in Table II. However, the outermost peaks do see a rather substantial shift, particularly the rightmost peak, which trends downwards from 9.60e-12 keV to -2.06e-11 keV.

We expect that the spectral dips on either end of the zero should occur at the same energy shift from each zero in velocity. However, this was not the case. As a result, the trends in energy shifts across temperatures are not constant. while the outermost peaks tend to shift downwards, the inner peaks remain constant, or even increase.

If it is true that the energy shifts are becoming lower, this means that the absorbed gamma rays are becoming more red-shifted as the absorber gets colder. This is behaving as we expected from Section I B. The resonant energies of the gamma rays decrease as the temperature gets colder due to the special relativistic time dilation at low temperatures as described in Equation 1.

C. Antiferromagnetism

We observed the Mössbauer spectra for FeF_2 at various different temperatures, and saw the transition to antiferromagnetism begin at 78K – instead of two peaks on either side of the velocity zero, it begins to split into four peaks. It properly completes the transition at 70K.

V. ACKNOWLEDGMENTS

Abstract: Sahar
Introduction: Sahar
Setup/Apparatus: Em and Sahar
Experiment: Em and Sahar
Conclusions: Sahar and Emme
Coding Graphs and Error Bars: Emmy
Pouring liquid nitrogen into a cryostat and feeling like a wizard: Sahar and Em
Singing along to Hadestown to cover the sound of the source rattling: Em and Sahar
Convincing the 4 PhD.'s to make liquid nitrogen ice cream with us: Sahar and Emm
The 4 PhD.'s in question, graciously making the liquid nitrogen ice cream: Joe Peidle, Matteo Mitrano, Jenny Hoffman, Jieping Fang

VI. APPENDIX

See all extra figures below.

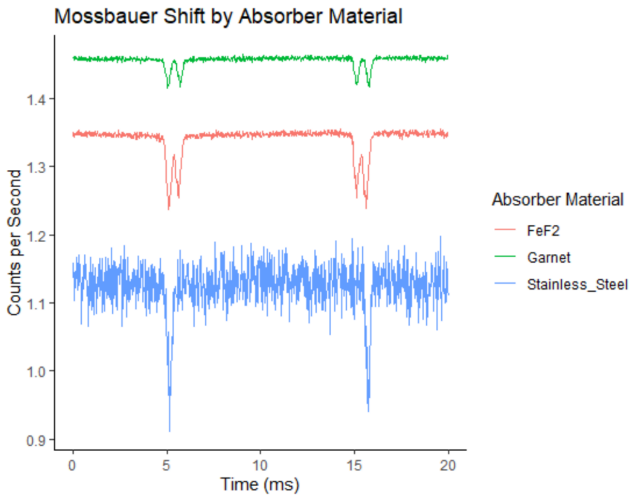

FIG. 8: Whole Mössbauer spectra of different absorber materials. Dips represent Doppler shifts at which the gamma rays had energies resonant with the material. Multipliers applied to order material lines: Garnet/1.5, FeF_2*1, Stainless Steel*1.05

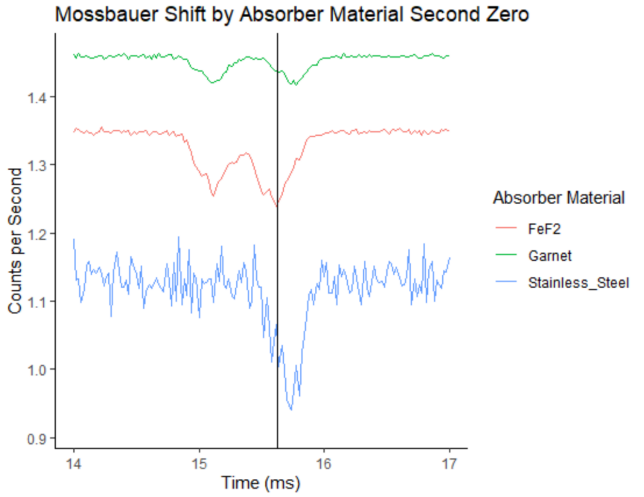

FIG. 9: Mössbauer spectra of different absorber materials. The black line is at time = 15.66 ms, the second zero of velocity of the loudspeaker based on the period of 20.875 ms. Dips represent Doppler shifts at which the gamma rays had energies resonant with the material. Multipliers applied to order material lines: Garnet/1.5, FeF_2*1, Stainless Steel*1.05

[1] L. Eyges, Physics of the mössbauer effect, American Journal of Physics **33**, 790 (1965).

[2] G. Vandegrift and B. Fultz, The mössbauer effect explained, American Journal of Physics **66**, 593 (1998).

[3] J. Hesse, Simple arrangement for educational mössbauer-effect measurements, American Journal of Physics **41**, 127 (1973).

[4] R. Weiner, Nuclear isomeric shift on spectral lines, Il Nuovo Cimento **4**, 1587 (1956).

[5] H. Lustig, The mössbauer effect, American Journal of Physics **29**, 1 (1961).

[6] G. P. Gupta and K. C. Lal, Temperature shift, recoil-free fraction, and force constant in mössbauer studies, Physica Status Solidi (b) **51**, 233 (1972).

Resonant Energy Shift by Absorber Material				
Material	energy shift 1 (keV)	energy shift 2	energy shift 3	energy shift 4
stainless steel	-1.64E-13	-	-4.57E-11	-
garnet	-5.19E-12	1.15E-10	1.20E-10	-4.07E-11
FeF_2	-1.64E-13	1.05E-10	1.10E-10	9.60E-12

TABLE I: The Mössbauer resonant energy shift for different absorber materials. The materials absorb more gamma rays at a small shift from the zero source velocity, at a small velocity and Doppler shift. Using Equation 4, these velocities were converted to the energy shift in the table. Adding 14.41 keV to each of these small shifts gives the resonant absorbtion energies. Stainless steel has only two peaks, one on each side of the source's zero velocity, while the other materials have four (two on each side).

Resonant Energy Shift for FeF_2 at Different Temperatures				
Temperatures	energy shift 1 (keV)	energy shift 2	energy shift 3	energy shift 4
300k	-1.64E-13	1.05E-10	1.10E-10	9.60E-12
190k	4.87E-12	1.15E-10	1.10E-10	4.57E-12
85k	-1.64E-13	1.40E-10	1.10E-10	-2.06E-11

TABLE II: The Mössbauer resonant energy shift for FeF_2 at different temperatures. The FeF_2 at each temperature absorbs more gamma rays at a small shift from the zero source velocity, at a small velocity and Doppler shift. Using Equation 4, these velocities were converted to the energy shift in the table. Adding 14.41 keV to each of these small shifts gives the resonant absorbtion energies. These are all the temperatures before the transition to antiferromagnetism at 78K.

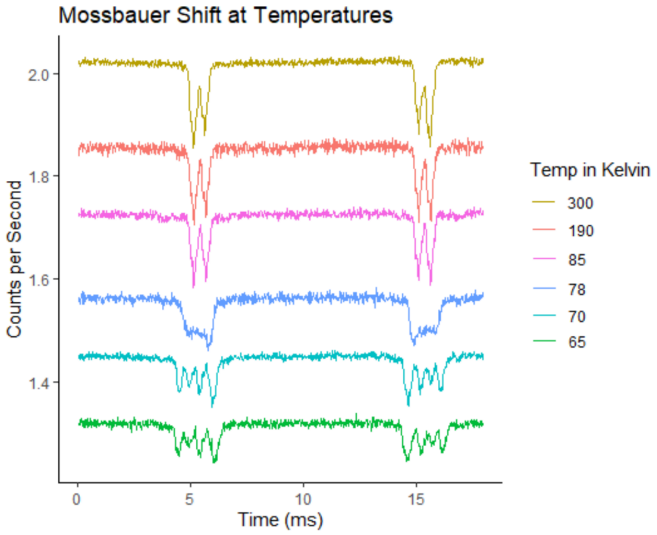

FIG. 10: Whole Mössbauer spectra of FeF_2 at different temperatures. Dips represent Doppler shifts at which the gamma rays had energies resonant with the material. Dips represent Doppler shifts at which the gamma rays had energies resonant with the material. Multipliers applied to order temperature lines: 300k*1.5, 190k*1.32, 85k*1.2, 78k*1.1, 70k/1.1, 65k/1.1.

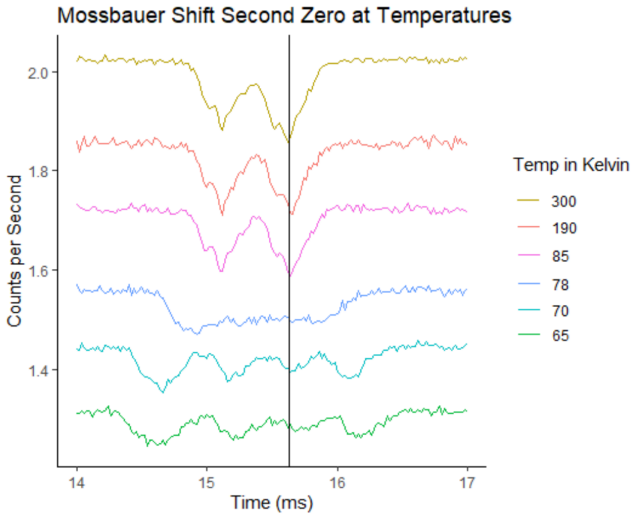

FIG. 11: Mössbauer spectra of FeF_2 absorber at different temperatures. The black line is at time = 15.66 ms, the second zero of velocity of the loudspeaker based on the period of 20.875 ms. Multipliers applied to order temperature lines: 300k*1.5, 190k*1.32, 85k*1.2, 78k*1.1, 70k/1.1, 65k/1.1.

[7] G. K. Wertheim, Temperature dependence of the fefs in fef below the néel temperature, Journal of Applied Physics **38**, 971 (1967).

[8] B. Henke, E. Gullikson, and J. Davis, X-ray interactions: photoabsorption, scattering, transmission, and reflection at e=50-30000 ev, z=1-92 (1993).